

Assessing the performance of NDVI as a proxy for plant biomass using non-linear models: a case study on the Kerguelen archipelago

H. Santin-Janin · M. Garel · J.-L. Chapuis ·
D. Pontier

Received: 7 July 2008 / Revised: 13 January 2009 / Accepted: 15 January 2009 / Published online: 25 February 2009
© Springer-Verlag 2009

Abstract Numerous ecological studies, including of the polar environment, are now using the remotely sensed normalized difference vegetation index (NDVI, e.g. PAL-NDVI or MODIS-NDVI) as a proxy of vegetation productivity rather than performing direct vegetation assessments. Even though previous data strongly suggested a saturation of NDVI at high biomass values, few studies have explicitly included this characteristic in the modelling process. Here, we developed a generalized non-linear model to explicitly model the relationship between temporal variations of NDVI (Pathfinder AVHRR Land 8 km dataset) and empirical field data. We illustrated our approach on the Kerguelen archipelago by using a green biomass index (point-intercept protocol) sampled at a small scale relative to PAL-NDVI data, and in presence of spatial (water) and temporal (cloud contamination, snow) heterogeneity, i.e. field conditions encountered in many ecological studies. We showed a strong relationship ($r_{\text{pred.obs}} = 0.89 [0.77; 0.95]_{95\%}$) between this index and the

seasonal component of NDVI time series (NDVI_{comp}). Despite the absence of lignified species in the stand, the NDVI_{comp} reached an asymptote (0.54 ± 0.05) for high values of green biomass index stressing the need to account for non-linearity when relating NDVI and plant measurements. We provided here a new methodological framework to standardize comparisons between studies assessing performance of NDVI as a proxy of vegetation data.

Keywords Generalized non-linear model · Negative binomial distribution · NDVI · Predictive model · Sub-antarctic · Validation study · Vegetation biomass

Introduction

Normalized difference vegetation index (NDVI) from remote sensors, most often onboard satellites, is now commonly used by ecologists as a proxy for vegetation productivity (Petturelli et al. 2005). Previous studies have related NDVI values and metrics derived from NDVI time series to different canopy attributes such as net primary production (NPP) (Tucker et al. 1981, 1983; Box et al. 1989; Paruelo et al. 1997), percentage of absorbed photosynthetically active radiations (APAR) (Asrar et al. 1984; Sellers et al. 1992), leaf area index (LAI) (Waring 1983; Tucker et al. 1986; Gilabert et al. 1996), evapotranspiration (Box et al. 1989) and plant biomass (Tucker et al. 1985; Diallo et al. 1991; Persson et al. 1993; Hobbs 1995). Based on such findings, NDVI has then been used to describe vegetation pattern (Sinclair et al. 1971; Tucker 1979; Aragón and Oesterheld 2008; Lobo et al. 2008), to explore ecosystem functioning (Lloyd 1990; Reed et al. 1994; Hunt et al. 1996; Mysterud et al. 2007) and responses to global changes (Penuelas and Filella 2001;

H. Santin-Janin (✉) · M. Garel · D. Pontier
Laboratoire de Biométrie et Biologie Évolutive,
Université de Lyon, Université Lyon 1, CNRS, UMR 5558,
43 boulevard du 11 novembre 1918, 69622 Villeurbanne, France
e-mail: hugues.sj@biomserv.univ-lyon1.fr

M. Garel
Office National de la Chasse et de la Faune Sauvage,
Centre National d'Étude et de Recherche Appliquée Faune de
Montagne, 95 rue Pierre Flourens, BP 74267,
34098 Montpellier Cedex 05, France

J.-L. Chapuis
Muséum National d'Histoire Naturelle,
Département Ecologie et Gestion de la Biodiversité,
Conservation des espèces, restauration et suivi des populations,
UMR 5173 MNHN-CNRS-P6, CP 53, 61 rue Buffon,
75005 Paris, France

Gong and Ho 2003; Guo et al. 2008), including arctic areas (Hope et al. 2005; Jia et al. 2006; Reynolds et al. 2008; Verbyla 2008).

Obtaining empirical vegetation data over large spatio-temporal scale is costly and time consuming. In sub-Antarctic area, this has so far been limited both by logistical constraints and by extreme climatic conditions often leading to short and local time series. As a consequence, numerous studies are now using NDVI as a proxy of vegetation productivity instead of performing direct vegetation assessments (e.g., Andersen et al. 2004; Garel et al. 2006; Pettorelli et al. 2007; Ryan et al. 2007; Tveraa et al. 2007; Wittemyer et al. 2007).

Studies focusing on the relationships between NDVI values and biophysical parameters put forward differences according to sites, stands and NDVI metrics (Goward et al. 1985; Tucker et al. 1985; Box et al. 1989; Hobbs 1995; Gilabert et al. 1996; Schino et al. 2003). This emphasizes the need to validate NDVI data before using it as a proxy of a vegetation productivity. These prior studies also reveal some discrepancies regarding the shape of these relationships [e.g., quadratic, log-linear, linear relationships between NDVI and vegetation biomass see Hobbs (1995), Gilabert et al. (1996), Schino et al. (2003), respectively]. However, due to the variety of the statistical approaches used, it remains unclear whether these discrepancies reveal true biological differences, such as differences in plant community characteristics, or methodological concerns. More specifically, NDVI is expected to saturate for high biomass values as it represents the greenness of the two dimensional covering of vegetation rather than plant biomass (Hobbs 1995). Such a process should lead to a non-linear relationship between NDVI and biomass data. However, few studies so far explicitly included this characteristic in the modelling process (e.g. Goward et al. 1985; Tucker et al. 1985; Schino et al. 2003), as they also often did not account for the non-normal distribution of the biophysical parameters studied.

The aim of our study was to provide a unified statistical framework for modelling the relationship between time variations of NDVI, and/or metrics derived from NDVI time series, and field vegetation data. We used an empirical generalised non-linear model that explicitly included the saturation of NDVI (i.e., without data transformation) to predict temporal variations in a green biomass index from NDVI time series of the Pathfinder Advanced Very High Resolution Radiometer (AVHRR) Land (PAL) 8 km resolution database. We illustrated our approach with a case study on a coastal area of the Kerguelen archipelago. We used field vegetation data based on “point intercept” principle. Methods using this principle have been commonly used in vegetation studies as a reliable linear proxy

of plant biomass (Jonasson 1988; Frank and McNaughton 1990; Bråthen and Hagberg 2004) and have been successfully applied for habitat monitoring of animals populations (e.g., Tixier et al. (1997) in roe deer *Capreolus capreolus*, Adrados et al. (2003) in red deer *Cervus elaphus*, Bråthen et al. (2007) in reindeer *Rangifer tarandus*). As also often encountered in polar environment and in many field studies, our vegetation data were sampled at a small spatial ($\sim 10 \text{ m}^2$) and temporal (3 years) scales relative to PAL-NDVI data (64 km^2), and on both spatially (water-vegetation, see Fig. 1) and temporally (cloud contamination, snow) heterogeneous pixels. In these conditions, we illustrated how our model can be used to assess the predicting power of NDVI times series on time variations of a green biomass index.

Materials and methods

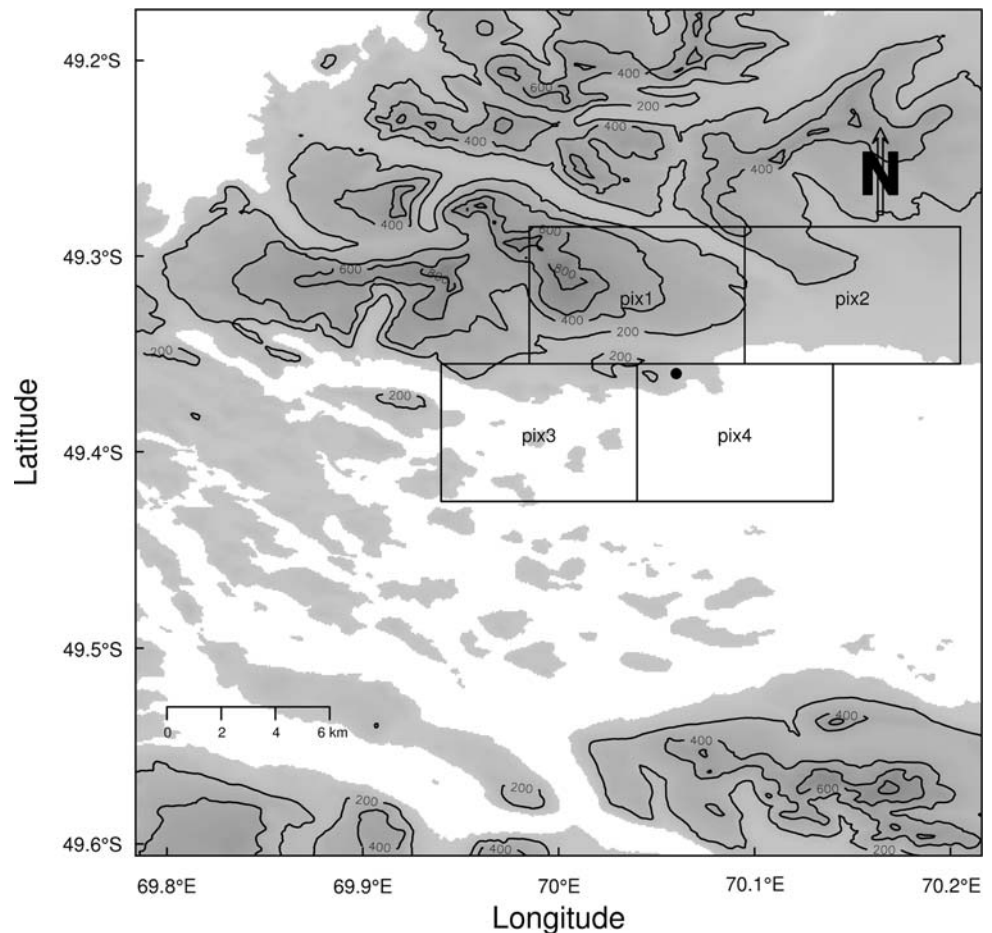
Study area

The study area (Molloy: 49.36° S–70.06° E, 0–150 m asl, Fig. 1) is located in “Baie du Morbihan” on the eastern part of the Grande Terre Island ($6,675 \text{ km}^2$), which is the main island of the Kerguelen archipelago.

Climatic conditions are cold, wet and windy. For the period 1977–1986, the average annual temperature was $4.9 \pm 0.2^\circ\text{C}$ (Météo-France, Port-aux-Français). For the same period, the precipitations occurred frequently (on average 187 ± 25 days per year) with a mean of $762 \pm 136 \text{ mm}$ per year. There is on average 53.9 ± 13.4 days with snow on the soil per year. Due to frequent (133 ± 20 days per year of wind greater than 24 m s^{-1}) and strong winds (monthly maximum average $45.8 \pm 3.8 \text{ m s}^{-1}$ but can reach up to 69 m s^{-1}), the nebulosity and water vapour concentrations remains high during most part of the year. The climate dynamics has an annual cycle (November–November, passing through the current January). We can distinguish two seasons per year: (1) the “Spring–Summer” from November to April and (2) the “Autumn–Winter” from May to October.

There were only non-lignified plant species on the Kerguelen archipelago. A large part of the study area was covered by an homogeneous stand of two perennial species, *Acaena magellanica* (Rosaceae) and *Taraxacum officinale* (Asteraceae). *A. magellanica* can reach 40 cm high and forms a very dense layer of vegetation (Boussès 1991). In summer the cover of *A. magellanica* is greater than 75% and the cover of *T. officinale* (commonly called Dandelion) was between 10 and 25%. Remaining parts of the study area were dominated by bare soil or were composed of small species (<10 cm, cover <10%) such as *Poa kerguelensis*, *P. annua*, *Ranunculus biternatus* or

Fig. 1 Location of the study site (black point) and of the four NDVI pixels (centre of pixel 1: 49.32°S–70.04°E, pixel 2: 49.32°S–70.15°E, pixel 3: 49.39°S–69.99°E, pixel 4: 49.39°S–70.09°E). Only pixels 3 and 4 are retained to perform the analysis but note that pooling the four pixels give qualitatively the same results. The Grande Terre Island of the Kerguelen archipelago is in light grey. Solid black lines represent contour lines



Sagina procumbens. Above 300 m asl, the vegetation is only present in form of small patches.

Data collection

Empirical field data (from Boussès 1991) were collected monthly (the day of the month of the survey was not available) in the field from February 1985 to February 1988, according to the point intercept protocol (Forgeard and Chapuis 1984). Three transects of 3.5 m long were randomly placed and delimited by wood sticks. Seventy points were evenly spaced 5 cm along the transect. A graduate stick of 100 cm was vertically lowered at each point. This stick was graduated by increment of 5 cm. The observers ($n = 3$) counted the presence of at least one contact between the focal species and the stick for each increment. The results were expressed as the total number of contacts over layers and transects for both *A. magellanica* and *T. officinale*. Based on previous studies we assumed that the time variations in numbers of intercept points is a linear proxy of time variation in green biomass (McNaughton 1979; Jonasson 1988; Frank

and McNaughton 1990; Boussès 1991; Bråthen and Hagberg 2004).

From the NOAA¹/NASA² PAL 8 km dataset archived at the Goddard Earth Sciences, Distributed Active Archive Center (GES-DAAC), we extracted the NDVI spanning the temporal resolution (month) of field data. Using monthly composite images contribute to reduce the amount of clouds and dust in the data (Holben 1986). Although this dataset was no longer available (acquisition period: 1981–2001), it was the only one freely and easily available for our study site and time period considered (see Agbu and James 1994; Pettorelli et al. 2005). For further details on the PAL data set and processing, see e.g., Agbu and James (1994).

As the study site is located in the top left corner of a NDVI pixel, we used the two lower nearby NDVI pixels (pixels 3 and 4) of this one to ensure that NDVI data were representative of the vegetated part of the study area (see Fig. 1). We have also performed the subsequent analyses

¹ National Oceanic and Atmospheric Administration.

² National Aeronautics and Space Administration.

using any combination of the four pixels including the study area (see Fig. 1) and have obtained qualitatively the same results (not presented here) as NDVI values were highly correlated among these 4 pixels (r from 0.94 to 0.97). These results corroborate the homogeneity of the study area and the spatial consistence of NDVI time series despite the presence of water in the pixels. Moreover, it suggests that the saturation of NDVI values (see “Results”) is not due to the presence of large water body in the two pixels used (pixels 3 and 4; see “Discussion”, and Chen 1999).

We have explored vegetation patterns by computing the NDVI (Reed et al. 1994; Myneni et al. 1995) based on Eq. 1:

$$\text{NDVI} = \frac{\rho_{\text{nir}} - \rho_{\text{red}}}{\rho_{\text{nir}} + \rho_{\text{red}}} \quad (1)$$

where ρ_{nir} and ρ_{red} are, respectively, the reflectance measurements in the red and the near infra-red part of the electromagnetic spectrum.

To reduce the effect on the data of both, atmospheric disturbances and spatial heterogeneity due to the presence of large water body in the two pixels used (Fig. 1), we computed an additional NDVI time series (called NDVI_{max}) by selecting the maximum NDVI value between these two pixels for each month (Holben 1986). Because a negative NDVI value means no vegetation activity, we replaced negative NDVI_{max} values ($n = 3$: -0.0008 , -0.0653 and -0.003) by 0 (Beck et al. 2006).

Statistical analyses

Empirical field data used in this study were sampled at a small scale relative to NDVI and at unknown date in the month. Moreover, field measurements were based on the two dominant species of the stand and were not randomly sampled within the NDVI pixel. Consequently, empirical field data cannot be used as true values of green biomass to calibrate NDVI data through a standard calibration approach (Osborne 1991). Instead, we used a predictive framework based on a generalized non-linear model to predict time variations in green biomass index from NDVI time series. We used the number of intercept points as response variable to explicitly model (error term, see Eq. 2) the unexplained variance in the field data (e.g., sampling error, mismatch in dates and scales, restricted sampling of plant community). Because NDVI time series were also partly affected by sampling error (water vapour or satellite drift), we applied smoothing algorithm on these data (as proposed by Reed et al. 1994) to account for discrepancies in the local trend with regard to vegetation phenology. We aimed here to improve the predictive power of NDVI data on time variations in green biomass index.

Quantifying the NDVI saturation trend

Our aim here was to provide a unified methodological framework accounting for previous findings which strongly suggested a non-linear relationship between NDVI and field measurements, with NDVI reaching a plateau for high biomass values (see also “Discussion”; Tucker et al. 1986; Hobbs 1995; Gilabert et al. 1996). We developed a saturation model including a restricted number of parameters biologically meaningful which should help to standardize between-study comparisons.

To quantify the saturation relationship between time variations in NDVI values and green biomass index measured in the field (see “Results”, Fig. 4), we developed a generalised non-linear model based on

$$y_i = \mu_i + \epsilon_i \quad (2)$$

with

$$\mu_i = \beta_0 + \frac{\beta_1 \times \text{NDVI}_i}{\beta_2 - \text{NDVI}_i} \quad (3)$$

where y_i is the number of intercept points at time i , β_0 the number of intercept points observed for a nil NDVI value (see “Discussion”), β_1 the increase rate in number of intercept points for a unity variation of NDVI values and $\frac{1}{\beta_2 - \text{NDVI}}$ a saturation term with β_2 the asymptotic NDVI value.

As often encountered with field biomass data, the variance of the number of intercept points increased faster than the mean ($\hat{\mu} = 201.18$, $\hat{\sigma}^2 = 31792.16$), leading us to make the assumption that the distribution of the intercept points could be approximated by a negative binomial distribution (Bliss and Fisher 1953):

$$y_i \sim \text{NegBin}(\mu_i, \theta) \quad (4)$$

leading to

$$\text{Var}(\epsilon_i) = \mu_i + \frac{\mu_i^2}{\theta} \quad (5)$$

where θ is an extra parameter of the negative binomial distribution which adjusts for the dispersion.

Based on the assumption that the response variable is independently distributed, we computed maximum likelihood estimates of $\{\beta_0, \beta_1, \beta_2, \theta\}$. This assumption remains valid as long as there is no autocorrelation in the residuals of a given model, as it is the case in this study (see “Results”). We implemented a function returning the log likelihood of the parameter estimation in R (R Development Core Team 2007, available upon request) and maximised it numerically using the function “optim” (Nelder and Mead method, Venables and Ripley 2002). To ensure that $\theta > 0$ we used a log transformation of this parameter in the likelihood function. We estimated the

respective standard errors of $\{\hat{\beta}_0, \hat{\beta}_1, \hat{\beta}_2, \hat{\theta}\}$ by taking the square root of the diagonal elements of the inverse Hessian matrix (Seber and Wild 1989).

Improving the predictive power of NDVI data

To reduce the effect of cloud contamination on NDVI values, i.e., to improve their predictive power on time variations in green biomass index, we applied two different algorithms on NDVI_{max} time series. First, we computed the NDVI_{smooth} time series using a non-linear running median line-smoother algorithm (Tukey 1977), as proposed by Reed et al. (1994). The median window was centred on each observation and had a length of three. The first and last values were computed using “Tukey’s end point rule”, i.e., $sm_i = \text{median}(y_i, sm_{i+1}, 3 \times sm_{i+1} - 2 \times sm_{i+2})$ where y_i is the i th element of the vector to be smoothed and sm is the smoothed one. This algorithm preserved the essence of the NDVI time series while eliminating much of the contaminated data. Second, we decomposed the NDVI_{max} time series with a moving average filter (Kendall and Stuart 1976; Malinvaud 1978; Ibanez et al. 2006) to extract the seasonal NDVI component (called NDVI_{comp}). We set the order of the moving average at 2 (the window of the average being $2 \times \text{order} + 1$), which corresponded to the last significant time lag of the autocorrelation function performed on NDVI_{max}. We computed the first and last values by filling them with the average of observations before applying the filter. This algorithm was less conservative than the non-linear running median line-smoother but was more flexible given that we specified the smoothing order.

Model selection and model validation

We used the Akaike’s Information Criterion adjusted for overdispersion and small sample size to perform model

selection among a set of three non-nested models including either NDVI_{max}, either NDVI_{smooth} or NDVI_{comp} as dependent variable (QAIC_c, Burnham and Anderson 2002). We re-estimated theta for each model (noted that the maximum likelihood estimate of theta among the different models were between 3.35 and 4.34). However, when we assessed the significance of the intercept (β_0) for the best selected model, we kept the theta constant as recommended by Venables and Ripley (2002). We assessed the predictive power of the model by computing the coefficient of correlation between predicted and observed values.

We evaluated the fit of the best model in two ways. First, we performed a χ^2 Goodness of fit test (GOF) to assess whether θ has been estimated properly. Second, we checked that the standardized residuals had a constant variance and were ranging between ± 2 . Then, we used both a parametric bootstrap and a Monte-Carlo procedure (Manly 1997; Efron and Tibshirani 1993) to assess the boundaries of the 95% prediction intervals (see Appendix).

Graphics and statistical analyses were performed with R 2.6.0 (R Development Core Team 2007) using the “MASS” (Venables and Ripley 2002), “pastecs” (Ibanez et al. 2006), “maps” (Brownrigg and Minka 2007) and “mapdata” (Brownrigg 2007) packages.

Results

Time variations in green biomass index

The survey of Molloy’s vegetation by the point intercept methodology yielded information about the time variations in green biomass of *A. magellanica* and *T. officinale* ($n = 27$ surveys; Fig. 2). Values were not available each month due to logistic and climatic constraints that limited

Fig. 2 Time variations in the number of intercept points for *A. magellanica* (dashed black line) and *T. officinale* (dashed grey line)

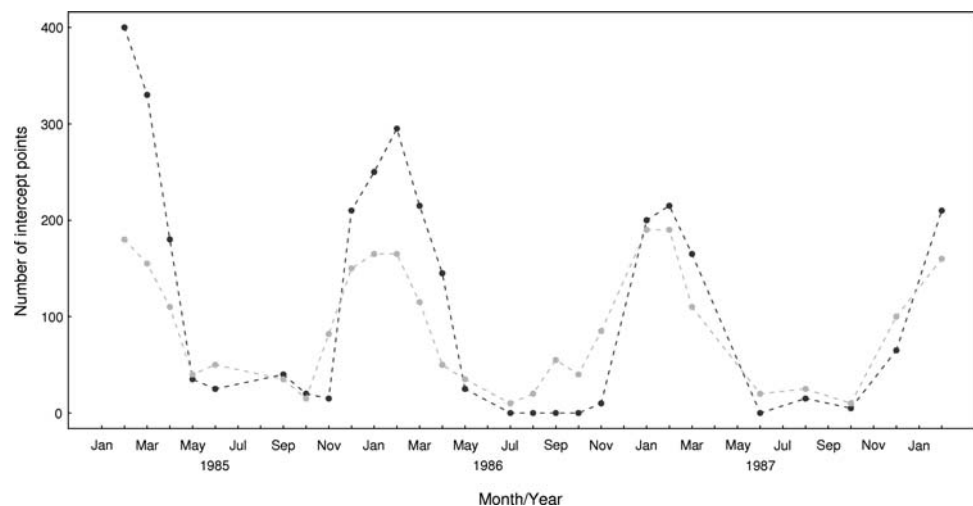


Fig. 3 Time variations in centred and scaled (mean = 0, variance = 1) time series of field measurements of total plant biomass (sum of intercept points of *A. magellanica* and *T. officinale*; black points) and centred and scaled NDVI measurements of the two pixels used in the analysis (pixel 3 solid grey line; pixel 4 solid black line)

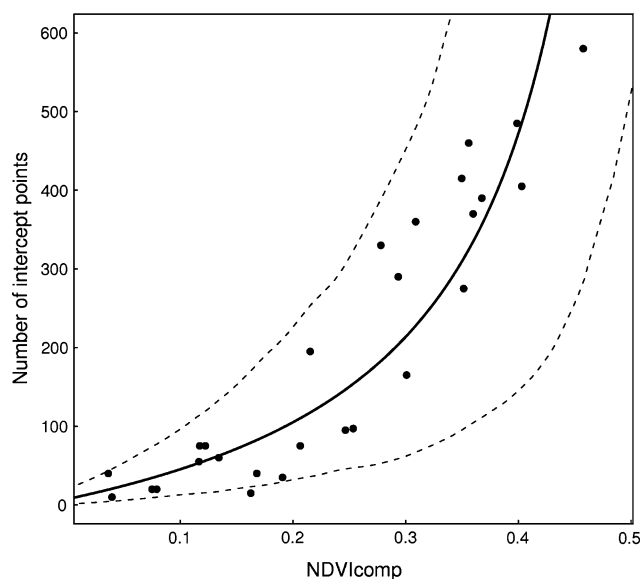
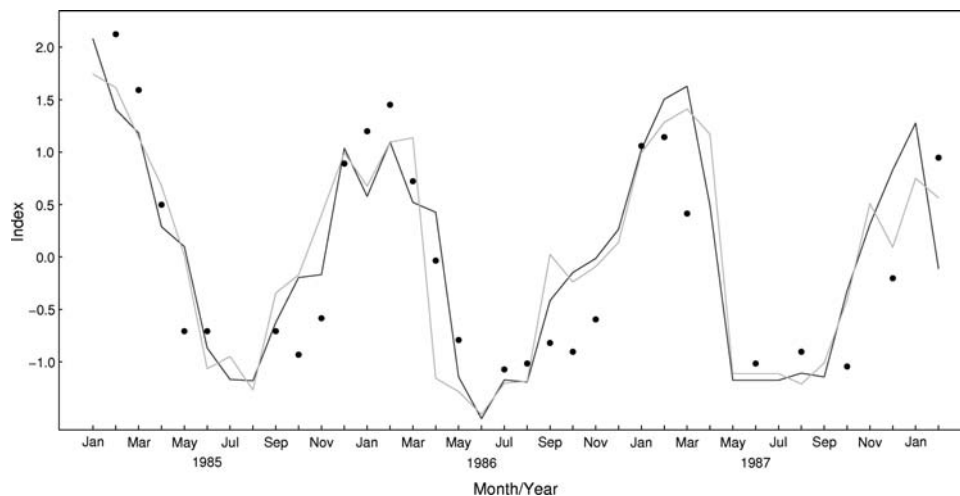


Fig. 4 Relationship between the total number of intercept points observed (sum of intercept points of *A. magellanica* and *T. officinale*) and the seasonal component of the NDVI ($NDVI_{comp}$) (black points). The solid line represents predictions of the non-linear model adjusted with $NDVI_{comp}$ (see text). The dashed lines represent 95% bootstrap prediction intervals (see Appendix)

the access to the study site. The number of intercept points ranged from 0 to 400 for *A. magellanica* and from 10 to 190 for *T. officinale*. Figure 2 shows the extensive development of *A. magellanica* occurring in December. At this period, it can reach 30–40 cm high in a few weeks (Boussès 1991). The development of *T. officinale* starts in October–November and precedes that of *A. magellanica*. To account for the variations in seasonal dynamics of the two species in further analyses, we took the sum of number of intercept points of both species for each time period as a proxy for time variations in total green biomass.

Relationship between NDVI and empirical field data

A good agreement was observed between the temporal variations of the two raw NDVI time series and the time variations in numbers of intercept points (Fig. 3). The time variations in numbers of intercept points observed and predicted from the non-linear model including $NDVI_{max}$ were strongly correlated ($r_{obs,pred} = 0.79$ [0.59;0.90]_{95%}; $QAIC_c = 98.64$). Although the data better supported a non-linear model including $NDVI_{smooth}$ instead of $NDVI_{max}$ ($QAIC_c = 88.76$; $r_{obs,pred} = 0.81$ [0.63;0.91]_{95%}), the best model included $NDVI_{comp}$ ($QAIC_c = 75.1$; $r_{obs,pred} = 0.89$ [0.77; 0.95]_{95%}; Figs. 4, 5, 6). Parameter estimates for the non-linear model including $NDVI_{comp}$ were: $\hat{\beta}_0 = 7.36$ (intercept), $\hat{\beta}_1 = 168.71$ (slope), $\hat{\beta}_2 = 0.54$ (NDVI asymptote), $\hat{\theta} = 4.54$ (dispersion parameter), and their respective standard errors was: 6.64, 47.13, 0.05, 1.33. Note that a non-linear model without intercept $\{\beta_1, \beta_2, \theta\}$, including $NDVI_{comp}$, gave a similar fit ($QAIC_c = 75.6$).

The goodness of fit test revealed that θ has been estimated properly ($\chi^2 = 24.56$; $df = 23$; $p = 0.37$). The standardized residuals of the $NDVI_{comp}$ model were not autocorrelated ($r_{lag1} = 0.23$; $df = 25$; $p = 0.24$) (Wey 1990), had a constant variance and ranged between -1.38 and 2.03 (except one, -3.44 , in February 1985). These results indicated that the non-linear model including $NDVI_{comp}$ fitted the data well, leading to a good agreement between the number of intercept points observed and predicted by this model (Fig. 6)

Discussion

By providing a unified statistical framework that explicitly account for saturation when relating NDVI and field measurements, our approach allows to standardize comparisons among studies and should thus help to understand

Fig. 5 Time variations in field measurements of total plant biomass observed (sum of the intercept points of *A. magellanica* and *T. officinale*; black points) and predicted by the non-linear model adjusted with $NDVI_{comp}$ (solid line; see text). The dashed lines represent 95% bootstrap prediction intervals (see Appendix)

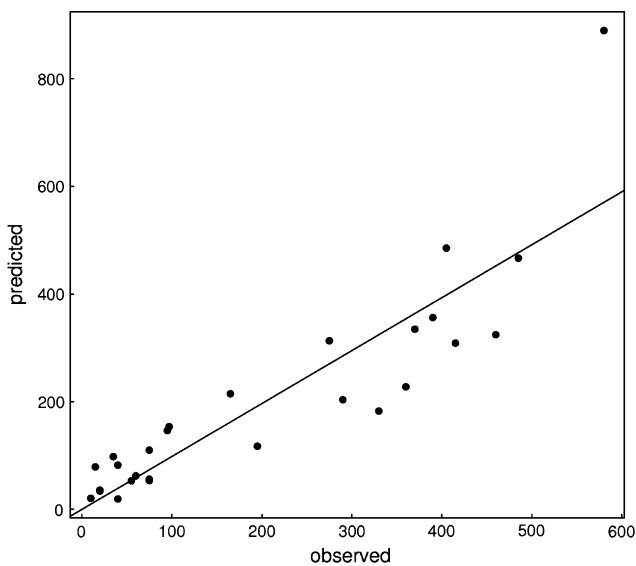
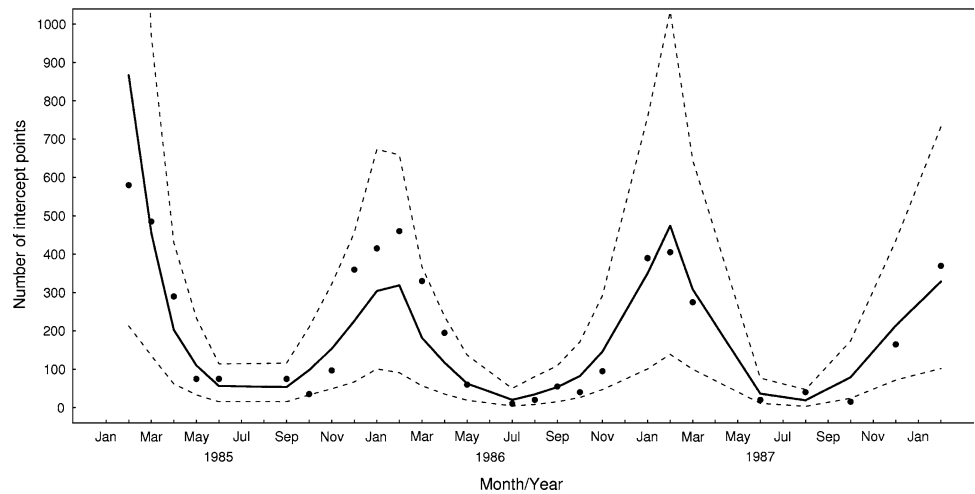


Fig. 6 Number of intercept points observed and predicted by the generalised non-linear model with $NDVI_{comp}$ as explanatory variable. The solid line represents the regression line of the linear model fitted with the number of intercept points predicted as the response variable and the number of intercept points observed as the explanatory variable

site-specific differences when assessing performance of NDVI as a proxy of vegetation data. Based on a generalised non-linear model, we were able to predict from both raw ($NDVI_{max}$) and processed ($NDVI_{smooth}$ and $NDVI_{comp}$) NDVI data a large part of the time variations (r^2 from 62 to 79%) in green biomass index of the two dominant plant species of the stand. Although our study was only based on temporal replicates, not spatial, which are likely to improve the performance of our model, this result is very encouraging. Indeed, it was obtained despite a restricted temporal dataset, large water body in the pixel and a large scale difference between field and satellite measurements which are “non-ideal” conditions often encountered in polar and

wildlife studies. We have shown that applying a moving average filter on NDVI time series reduces the effect of temporal heterogeneity mainly caused by variations in atmospheric conditions. However, in area where such problems are limited, this method should be used with caution as it may reduce the NDVI peaks in the curves, which are assumed to be valid NDVI values, leading to overlook important ecological variability (Reed et al. 1994).

The need to account for non-linearity

Our approach explicitly models the non-linear nature of the relationship between time variations of NDVI values and green biomass index suggested by previous validation studies (Tucker et al. 1981, 1983; Goward et al. 1985; Paruelo et al. 1997 but see Box et al. 1989). Tucker et al. (1986) have demonstrated a consistent functional relationship between LAI and spectral vegetation index derived from satellite measurements, where NDVI had an obvious tendency to reach a plateau at high LAI levels. The shape of the relationship indicated a temporary saturation of reflectance, which disappears with the subsequent senescence of the foliage (Gilabert et al. 1996). This suggests that NDVI values systematically underestimate the green biomass of stand with high production of green biomass and strong foliage density.

We estimated an asymptotic NDVI value (0.54) greater than the one (0.40) used by Box et al. (1989) who based their study on Net Primary Production measurements coming from different biomes including highly structured ones such as equatorial rainforests. Thus, our result also strongly supports the need to rely on non-linear model when relating NDVI and field measurements, and as a consequence the need of caution when using NDVI as a linear proxy of vegetation productivity without validation. As there is no arborescent or shrubby layer on the

Kerguelen archipelago, we can explain this rapid saturation of NDVI by the strong foliage density of *A. magellanica*. The monthly resolution of NDVI data probably also contributes to this result. Indeed, the compositing procedure of PAL-NDVI data is based on the selection of the maximum NDVI bin (see Agbu and James 1994). Thus, during the growing season, if the field measurements occurred at the beginning of the month, it is likely that the NDVI bin retained was the one corresponding to the end of the month, i.e., the NDVI value was representative of a higher green biomass than the one measured in the field. Using satellite data with a higher temporal resolution should reduce this phenomenon because it will reduce the delay between acquisition date of field and satellite measurements.

Relating NDVI and biomass data in subantarctic environment

The study reported here also raises issues of different technical refinements and specificity when relating NDVI and field measurements which might be encountered in multiple field studies and in particular in subantarctic environment. First, if there is no green biomass, the NDVI value is expected to equal zero and the curve fitted should therefore pass by the zero point (Fig. 4). However, we estimated an intercept (Eq. 3) because field measurements were only based on the two main species of the stand (Boussès 1991). This suggests that a zero intercept point value would not necessarily correspond to a zero NDVI value. We therefore expected a negative intercept ($\hat{\beta}_0$). Nevertheless, we obtained a positive estimation of the intercept ($\hat{\beta}_0$) that could be explained by the temporary occurrence of snow in the pixel, which has a differential influence on satellite than on the field measurements. For example, if the soil is largely covered by snow, the satellite measurement will converge to zero. Due to special exposition or topography conditions, some parts of the pixel are likely to be locally free of snow. This could influence the field but not the satellite measurements if the area concerned is smaller than the nominal resolution of the satellite Field Of View (1.1 km for AVHRR data). Here, the intercept ($\hat{\beta}_0$) did not significantly improve the fit of the model, suggesting that in our case the presence of snow and other species had a negligible effect on the shape of the relationship between time variations of $\text{NDVI}_{\text{comp}}$ and green biomass index (see Fig. 4).

Second, a major problem for validating satellite measurements is to scale biophysical parameters from the plot to larger scales. In this study, we compared NDVI time series at 8 km × 8 km spatial resolution, with empirical field measurements coming from three transects of 3.5 m long (~10 m²). In our case, however, the limitation due to

very high spatial resolution of empirical field measurements could be overcome by the relative homogeneity of the vegetal stand. This is corroborated by the similarity of the four NDVI time series (see Fig. 3 and “Materials and methods”). Moreover, the presence of sea water in the NDVI pixels is likely to increase their spatial resolution. This is related to the binning process of AVHRR data, which retained the maximum NDVI value (see Agbu and James 1994). Indeed, because here the greenness intensity is likely greater on land than on water, the NDVI values retained are more likely representative of a vegetated area smaller than 64 km².

Third, atmospheric conditions such as cloud cover and/or aerosols have a strong influence on NDVI values due to differential effect of water vapour on measurements performed by the red and near infra-red channels of the radiometer (Forster 1984; Holben 1986; Gutman 1991). The compositing process based on the maximum NDVI value removes a large part but not all the contamination of NDVI data by atmospheric conditions. For instance, in January 1986, from September to December 1986, and in December 1987, NDVI time series were steady or decreased, despite a local rising trend (see Fig. 3). Under the assumption that NDVI fluctuations represent time variations in green biomass index, the discrepancies of NDVI values regarding the local trend cannot be related to a decrease in green biomass because they appeared during the developmental phase of the vegetation dynamics. However, the extreme climatic conditions that occurred on the Kerguelen archipelago (see “Materials and methods”) could explain these unexpected NDVI values. As proposed by Reed et al. (1994), smoothing NDVI time series ($\text{NDVI}_{\text{smooth}}$) improves the intensity of the relationship between time variations of green biomass index and NDVI, but irregularities are still present, especially for January 1986. However, using the seasonal component of NDVI time series ($\text{NDVI}_{\text{comp}}$) to predict time variations in green biomass index provided better results than $\text{NDVI}_{\text{smooth}}$.

Conclusion

The originality of our study resides in the presentation of a new and general modelling approach to relate NDVI and field vegetation data that explicitly includes the saturation of NDVI suggested by previous studies (Tucker et al. 1986; Hobbs 1995; Gilabert et al. 1996). Our model does not require the use of variable transformation and relies on biologically meaningful parameters. We thereby provides a way to standardize comparison between studies investigating the saturation of NDVI data in contrasted environmental conditions. Our study is also the first

validation of NDVI data in a subantarctic ecosystem and should be of great interest for scientists using NDVI in subantarctic environment and more generally in ecological studies, as it reinforces the idea that NDVI is most often a non linear proxy of plant biomass. Finally, although we show that NDVI was a good proxy of time variations in green biomass, further studies are required to assess the generality of such results for subantarctic environments.

Acknowledgments We thank the French Polar Institute Paul-Emile Victor (IPEV) for financial support (programmes 279 and 136). Many thanks are due to J.-M. Gaillard, P. Aubry, R. Ecochard, M.-L. Delignette-Muller, I. Herfindal, J.-D. Lebreton, A. Avril and S. Hamel for their helpful suggestions on an earlier version of the manuscript. We also thank N. G. Yoccoz, S. Ryan and one anonymous referee for their comments that greatly improve the manuscript.

Appendix

This appendix describes the 3 steps of the statistical procedure used to compute prediction intervals of the model presented in this study (see Eqs. 2, 3),

Step 1: Computation of the mean model predictions

We obtained maximum likelihood estimation of $\{\beta_0, \beta_1, \beta_1, \theta\}$ noted $\{\hat{\beta}_0, \hat{\beta}_1, \hat{\beta}_1, \hat{\theta}\}$ and computed the means $(\hat{\mu}_i)$ predicted by the fixed part of the model:

$$y_i \sim \text{NegBin}(\hat{\mu}_i, \hat{\theta}) \tag{6}$$

where

$$\hat{\mu}_i = \hat{\beta}_0 + \frac{\hat{\beta}_1 \text{NDVI}_i}{\hat{\beta}_2 - \text{NDVI}_i} \tag{7}$$

Step 2: Parametric bootstrapping of the fixed part of the model

We computed 1,000 vectors of bootstrap observations of length $n = 27$,

$$Q^{*j}[\mu_1^{*j}, \mu_i^{*j}, \dots, \mu_n^{*j}]_{(1 \leq j \leq 1,000)} \tag{8}$$

where each μ_i^{*j} was sampled in

$$\text{NegBin}(\hat{\mu}_i, \hat{\theta}) \tag{9}$$

We fitted the non-linear model (see Eq. 2) on each Q^{*j} to obtain 1,000 bootstrap vectors of parameter estimations,

$$\{\hat{\beta}_0^{*j}, \hat{\beta}_1^{*j}, \hat{\beta}_2^{*j}, \hat{\theta}^{*j}\}_{(1 \leq j \leq 1,000)} \tag{10}$$

Using Eq. 7, we computed the 1,000 bootstrap vectors of predictions,

$$\hat{P}^{*j}[\hat{\mu}_1^{*j}, \hat{\mu}_i^{*j}, \dots, \hat{\mu}_n^{*j}]_{(1 \leq j \leq 1,000)} \tag{11}$$

Then, to compute the 95% bootstrap confidence intervals of the i th predicted mean $(\hat{\mu}_i)$, we have taken

the 0.025 and 0.975 quantiles of the corresponding $\hat{\mu}_i^*$ bootstrap distribution.

Step 3: Monte Carlo generation of the posterior distribution of individual predictions

In order to obtain the 95% prediction intervals, we included the random part of the model in the bootstrap procedure. Thus, we had a noise (Negative Binomial) to the 1000 bootstrap vectors of predicted means $(\hat{P}^{*j}$, see Eq. 11) to take into account the individual variability,

$$\hat{P}^{*j}[\hat{y}_1^{*j}, \hat{y}_i^{*j}, \dots, \hat{y}_n^{*j}]_{(1 \leq j \leq 1,000)} \tag{12}$$

where each \hat{y}_i^{*j} (see Eq. 2) was sampled in

$$\text{NegBin}(\hat{\mu}_i^{*j}, \hat{\theta}^{*j}) \tag{13}$$

Then, to compute the 95% bootstrap prediction interval of the i th predicted observation (\hat{y}_i) , we took the 0.025 and 0.975 quantiles of the corresponding \hat{y}_i^* bootstrap distribution.

References

Adrados C, Verheyden-Tixier H, Cargnelutti B, Pépin D, Janeau G (2003) GPS approach to study fine-scale site use by wild red deer during active and inactive behaviors. *Wildl Soc Bull* 31:544–552

Agbu P, James M (1994) The NOAA/NASA Pathfinder AVHRR Land data set user’s manual. Goddard Distributed Active Archive Center Greenbelt, Maryland

Andersen R, Herfindal I, Sæther B.-E, Linnell J, Odden J, Liberg O (2004) When range expansion rate is faster in marginal habitats. *Oikos* 107:210–214

Aragón R, Oesterheld M (2008) Linking vegetation heterogeneity and functional attributes of temperate grasslands through remote sensing. *Appl Veg Sci* 11:117–130

Asrar G, Fuchs M, Kanemasu E, Hatfield J (1984) Estimating absorbed photosynthetic radiation and leaf area index from spectral reflectance in wheat. *Agron J* 76:300–306

Beck P, Atzberger C, Høgda K, Johansen B, Skidmore A (2006) Improved monitoring of vegetation dynamics at very high latitudes: a new method using MODIS NDVI. *Remote Sens Environ* 100:321–334

Bliss C, Fisher R (1953) Fitting the negative binomial distribution to biological data. *Biometrics* 9:176–200

Boussès P (1991) Biologie de population d’un vertébré phytophage introduit, le lapin (*Oryctolagus cuniculus*) dans les îles subantarctiques de Kerguelen. Ph.D. thesis, Université de Rennes I, France

Box E, Holben B, Kalb V (1989) Accuracy of the AVHRR vegetation index as a predictor of biomass, primary productivity and net CO₂ flux. *Vegetatio* 80:71–89

Brownrigg R (2007) mapdata: extra map databases (R code). R package version 2.0–22

Brownrigg R, Minka T (2007) maps: draw geographical maps (R code). R package version 2.0–38

Bråthen K, Hagberg O (2004) More efficient estimation of plant biomass. *J Veg Sci* 15:653–660

Bråthen K, Ims R, Yoccoz N, Fauchald P, Tveraa T, Hausner V (2007) Induced shift in ecosystem productivity? Extensive scale effects of abundant large herbivores. *Ecosystems* 10:773–789

- Burnham K, Anderson D (2002) Model selection and multimodel inference: a practical information–theoretical approach, 2nd edn. Springer, New York
- Chen J (1999) Spatial scaling of a remotely sensed surface parameter by contexture. *Remote Sens Environ* 69:30–42
- Diallo O, Diouf A, Hanan N, Ndiaye A, Prevost Y (1991) AVHRR monitoring of savanna primary production in Senegal, West Africa. 1987–1988. *Int J Remote Sens* 12:1259–1279
- Efron B, Tibshirani R (1993) An introduction to the Bootstrap. volume 57 of monographs on statistics and applied probability. Forgeard F, Chapuis J-L (1984) Impact du lapin de garenne, *Oryctolagus cuniculus*, sur la végétation des pelouses incendiées de Paimpont (Ille-et-Vilaine, France). *Acta Oecol* 5:215–228
- Forster B (1984) Derivation of atmospheric correction procedures for LANDSAT MSS with particular reference to urban data. *Int J Remote Sens* 5:799–818
- Frank D, McNaughton S (1990) Above-ground biomass estimation with the canopy intercept method—a plant-growth form caveat. *Oikos* 57:57–60
- Garel M, Solberg E, Sæther B-E, Herfindal I, Høgda K (2006) The length of growing season and adult sex ratio affect sexual size dimorphism in moose. *Ecology* 87:745–758
- Gilabert M, Gandia S, Melia J (1996) Analyses of spectral-biophysical relationships for a corn canopy. *Remote Sens Environ* 55: 11–20
- Gong D, Ho C (2003) Detection of large-scale climate signals in spring vegetation index (Normalized Difference Vegetation Index) over the Northern Hemisphere. *J Geophys Res* 108:4498
- Goward S, Tucker C, Dye D (1985) North American vegetation patterns observed with the NOAA-7 advanced very high resolution radiometer. *Plant Ecol* 64:3–14
- Guo W, Yang T, Dai J, Shi L, Lu Z (2008) Vegetation cover changes and their relationship to climate variation in the source region of the Yellow River, China, 1990–2000. *Int J Remote Sens* 29: 2085–2103
- Gutman G (1991) Vegetation indices from AVHRR—an update and future prospects. *Remote Sens Environ* 35:121–136
- Hobbs T (1995) The use of NOAA-AVHRR NDVI data to assess herbage production in the arid rangelands of Central Australia. *Int J Remote Sens* 16:1289–1302
- Holben B (1986) Characteristics of maximum-value composite images from temporal AVHRR data. *Int J Remote Sens* 7: 1417–1434
- Hope A, Engstrom R, Stow D (2005) Relationship between AVHRR surface temperature and NDVI in Arctic tundra ecosystems. *Int J Remote Sens* 26:1771–1776
- Hunt E, Piper S, Nemani R, Keeling C, Otto R, Running S (1996) Global net carbon exchange and intra-annual atmospheric CO₂ concentrations predicted by an ecosystem process model and three-dimensional atmospheric transport model. *Glob Biogeo Cycles* 10:431–456
- Ibanez F, Grosjean P, Etienne M (2006) pastecs: package for analysis of space–time ecological series. R package version 1.3–4
- Jia G, Epstein H, Walker D (2006) Spatial heterogeneity of tundra vegetation response to recent temperature changes. *Glob Change Biol* 12:42–55
- Jonasson S (1988) Evaluation of the point intercept method for the estimation of plant biomass. *Oikos* 52:101–106
- Kendall M, Stuart A (1976) The advanced theory of statistics, vol 3. Design and analysis, and time-series. Griffin, London
- Lloyd D (1990) A phenological classification of terrestrial vegetation cover using shortwave vegetation index imagery. *Int J Remote Sens* 11:2269–2279
- Lobo A, Moloney K, Chic O, Chiariello N (2008) Analysis of fine-scale spatial pattern of a grassland from remotely-sensed imagery and field collected data. *Landsc Ecol* 13:111–131
- Malinvaud E (1978) Méthodes statistiques de l'économétrie, 3rd edn. Bordas, Paris
- Manly B (1997) Randomization, Bootstrap and Monte Carlo Methods in biology. Chapman and Hall, London
- McNaughton S (1979) Grassland–herbivore dynamics. In: Serengeti (ed) Dynamics of an ecosystem. University of Chicago Press, Chicago, pp 46–81
- Myneni R, Hall F, Sellers P, Marshak A (1995) The interpretation of spectral vegetation indexes. *IEEE Trans Geosci Rem Sens* 33:481–486
- Mysterud A, Tryjanowski P, Panek M, Pettorelli N, Stenseth N (2007) Inter-specific synchrony of two contrasting ungulates: wild boar (*Sus scrofa*) and roe deer (*Capreolus capreolus*). *Oecologia* 151:232–239
- Osborne C (1991) Statistical calibration—a review. *Int Stat Rev* 59:309–336
- Paruelo J, Epstein H, Lauenroth W, Burke I (1997) ANPP estimates from NDVI for the Central Grassland Region of the United States. *Ecology* 78:953–958
- Penuelas J, Filella I (2001) Phenology—responses to a warming world. *Science* 294:793–794
- Persson P, Hallkonyves K, Sjostrom G, Pinzke S (1993) NOAA AVHRR data for crop productivity estimation in Sweden. *Adv Space Res* 13:111–116
- Pettorelli N, Pelletier F, Von Hardenberg A, Festa-Bianchet M, Côté S (2007) Early onset of vegetation growth vs. rapid green-up: impacts on juvenile mountain ungulates. *Ecology* 88:381–390
- Pettorelli N, Vik J, Mysterud A, Gaillard J-M, Tucker C, Stenseth N (2005) Using the satellite-derived NDVI to assess ecological responses to environmental change. *Trends Ecol Evol* 20:503–510
- R Development Core Team (2007) R: a language and environment for statistical computing. R Foundation for Statistical Computing Vienna, Austria
- Raynolds M, Comiso J, Walker D, Verbyla D (2008) Relationship between satellite-derived land surface temperatures, arctic vegetation types, and NDVI. *Remote Sens Environ* 112:1884–1894
- Reed B, Brown J, Vanderzee D, Loveland T, Merchant J, Ohlen D (1994) Measuring phenological variability from satellite imagery. *J Veg Sci* 5:703–714
- Ryan S, Knechtel C, Getz W (2007) Ecological cues, gestation length and birth timing in African Buffalo (*Syncerus caffer*). *Behav Ecol* 18:635–644
- Schino G, Borfecchia F, De Cecco L, Dibari C, Iannetta M, Martini S, Pedrotti F (2003) Satellite estimate of grass biomass in a mountainous range in central Italy. *Agrofor Syst* 59:157–162
- Seber G, Wild C (1989) Nonlinear regression. Wiley, New York
- Sellers P, Heiser M, Hall F (1992) Relations between surface conductance and spectral vegetation indexes at intermediate (100 m² to 15 km²) length scales. *J Geophys Res* 97:19033–19059
- Sinclair T, Hoffer R, Schreiber M (1971) Reflectance and internal structure of leaves from several crops during a growing season. *Agron J* 63:864–868
- Tixier H, Duncan P, Scehovic J, Yani A, Gleizes M, Lila M (1997) Food selection by European roe deer (*Capreolus capreolus*): effects of plant chemistry, and consequences for the nutritional value of their diets. *J Zool (Lond)* 242:229–245
- Tucker C (1979) Red and photographic infrared linear combinations for monitoring vegetation. *Remote Sens Environ* 8:127–150
- Tucker C, Holben B, Elgin J (1981) Remote-sensing of total dry-matter accumulation in winter-wheat. *Remote Sens Environ* 11:171–189
- Tucker C, Justice C, Prince S (1986) Monitoring the grasslands of the Sahel 1984–1985. *Int J Remote Sens* 7:1571–1581

- Tucker C, Vanpraet C, Boerwinkel E, Gaston A (1983) Satellite remote-sensing of total dry-matter production in the Senegalese Sahel. *Remote Sens Environ* 13:461–474
- Tucker C, Vanpraet C, Sharman M, Vanittersum G (1985) Satellite remote-sensing of total herbaceous biomass production in the Senegalese Sahel—1980–1984. *Remote Sens Environ* 17:233–249
- Tukey J (1977) *Exploratory data analysis*. Addison-Wesley, Massachusetts
- Tveraa T, Fauchald P, Yoccoz N, Ims R, Aanes R, Høgda K (2007) What regulate and limit reindeer populations in Norway? *Oikos* 116:706–715
- Venables W, Ripley B (2002) *Modern applied statistics with S*. Springer, New York
- Verbyla D (2008) The greening and browning of Alaska based on 1982–2003 satellite data. *Glob Ecol Biogeogr* 17:547–555
- Waring R (1983) Estimating forest growth and efficiency in relation to canopy leaf-area. *Adv Ecol Res* 13:327–354
- Wey W (1990) *Time series analyses*. Addison-Wesley, Massachusetts
- Wittemyer G, Rasmussen H, Douglas-Hamilton I (2007) Breeding phenology in relation to NDVI variability in free-ranging African elephant. *Ecography* 30:42–50